ORIGINAL ARTICLE e-ISSN: 2349-0659 p-ISSN; 2350-0964

Antimalarial Activity of Eco-friendly Green Synthesis of Gold Nanoparticles Using *Coccinia grandis* (L.) Voigt. against *Plasmodium berghei*

Karunanithi Anbarasan[1], Abdul Abduz Zahir[1]*, Venkatesan Karthick[1], Abdul Abdul Rahuman[1], Kokati Venkata Bhaskara Rao[2]

Abstract

Malaria is one of the life-threatening infectious diseases caused by the *Plasmodium* parasites infect red blood cells of humans. The major problem associated with malaria treatment and control is the spread and development of resistance against chemical insecticides. Hence, the plant-based formulations may serve as an alternative source for the development of new drugs for the treatment of malaria. The present study is an attempt to evaluate the antiplasmodial activity of synthesized gold nanoparticles (Au NPs) using the aqueous leaves extract of *Coccinia grandis* against *Plasmodium berghei* and characterized by UV-Visible (UV-Vis) spectroscopy, Fourier transform infrared, X-ray diffraction, Scanning electron microscopy with Energy dispersive X-ray spectroscopy, and Transmission electron microscopy (TEM) with selected area (electron) diffraction analyzes. The UV-Vis spectra of Au NPs showed a surface plasmon resonance peak range of 500–600 nm. The TEM image revealed the spherical shape with a mean particle size of 2.82 ± 2.5 nm. The *in vivo* antimalarial activity of synthesized Au NPs showed a significant ($P < 0.001$) chemosuppressive effect, with parasite suppression of 88.75%, compared to aqueous extracts of *C. grandis* showed 69.45% against *P. berghei* at 100 mg/kg body weight. To sum up, further phytochemical research is required in the future to standardize *C. grandis* compounds with strong antiplasmodial activity and devise the best alternative nano herbal formulation to replace the synthetic drugs currently in use.

Keywords: Antimalarial, *Artemia salina, Coccinia grandis*, Synthesized gold nanoparticles, Transmission electron microscopy

Asian Pac. J. Health Sci., (2022); DOI: 10.21276/apjhs.2022.9.1.38

Introduction

Malaria is known as an acute febrile illness in endemic areas, and the most infectious disease with 228 million cases worldwide and 405,000 malaria deaths in 2018 with children under 5 years of age.[1] The World Health Organization (WHO) reported that there were an estimated 219 million malaria cases and 435,000 related deaths in 2017 and in India 4% of the global malaria burden and contributes 87% of the total malaria cases in Southeast Asia. However, several challenges have emerged in recent years which pose a threat to the country's progress in its fight against malaria. These include the development of malaria multi-drug resistance, insecticide resistance, and rapid urbanization leading to the emergence of malaria in urban areas, increased people migration, and climate change.[2,3] All these factors can seriously basket the country's malaria control efforts and therefore warrant imperative attention. In order to analyze these challenges, this requires a constant effort to explore new drugs, mainly with novel modes of action.

In the earlier reports, the synthesis of nanoparticles (NPs) using plant extracts has evolved into an essential branch of nanotechnology because of its perspective application in biomedical, magnetic and energy science. Huge amounts of synthesized NPs can be prepared easily using plants and the maximum of these are non-toxic.[4-6] Enormous attention focused in current years on the synthesis of gold NPs (Au NPs) because of their unique optoelectronic properties, their applications in catalysis, biotechnology and drug delivery.[7] The ability of Au NPs to strongly bind with biological molecules is being used to target tissues by conjugating the NPs surface with appropriate biomolecules.[8] Au NPs have gained increasing interest due to their electronic properties and extraordinary optical, high stability and biological compatibility, controllable morphology and size dispersion, and easy surface functionalization.[9] A significant attribute of Au NPs is their stability against oxidation and degradation *in vivo* study and these appealing properties are critical in the development of nanomaterials for use as clinical therapeutics and diagnostic tools.[10]

Numerous techniques, such as photochemical, electrochemical, chemical, radiation and biological, have been used for the biosynthesis of Au NPs.[11] Biological methods for NPs synthesis using microorganisms, enzymes and plant extracts have been focused on as possible eco-friendly alternatives to chemical and physical methods.

[1]Unit of Nanotechnology and Bioactive Natural Products, Post Graduate and Research Department of Zoology, C. Abdul Hakeem College (Autonomous), Melvisharam - 632 509, Ranipet District, Affiliated to Thiruvalluvar University, Vellore, Tamil Nadu, India.

[2]Department of Biomedical Sciences, Marine Biotechnology Laboratory, School of Biosciences and Technology, VIT University, Vellore, Tamil Nadu, India.

Corresponding Author: Dr. A. Abduz Zahir, Unit of Nanotechnology and Bioactive Natural Products, Post Graduate and Research Department of Zoology, C. Abdul Hakeem College (Autonomous), Melvisharam - 632 509, Ranipet District, Affiliated to Thiruvalluvar University, Vellore, Tamil Nadu, India. Tel.: +91-9789293183. E-mail: abduzzahir1984@gmail.com

How to cite this article: Anbarasan K, Zahir AA, Karthick V, Rahuman AA, Rao KV. Antimalarial Activity of Eco-friendly Green Synthesis of Gold Nanoparticles Using *Coccinia grandis* (L.) Voigt. against *Plasmodium berghei*. Asian Pac. J. Health Sci., 2022;9(1):148-155.

Source of support: Nil.

Conflicts of interest: None.

Received: 22/10/21 **Revised:** 11/11/21 **Accepted:** 02/12/21

The growing demand to produce safe processes for the synthesis of NPs without utilizing toxic chemicals. Thus, there is a need for "green chemistry" that includes a clean, non-toxic and environment-friendly method of NPs synthesis.[12] Earlier studies reported that the biosynthesized Au NPs using plant extracts of *Cassia auriculata*,[13] *Trianthema decandra*,[14] *Ricinus communis*,[15] *Mimosa tenuiflora*,[16] *Saraca indica*,[17] and *Couroupita guianensis*[18] and their activities such as antidiabetic, antimicrobial, anticancer, cytotoxicity, catalytic activities, and antiplasmodial activity, respectively.

Coccinia grandis (L.) Voigt., also known as "Ivy gourd" is a climbing perennial herb, is a member of the Cucurbitaceae family. It has been found in many countries such as Asia and Africa. The whole plant of *C. grandis* is used to treat allergy, bronchitis, jaundice, syphilis, gonorrhoea, fever, indigestion, nausea, eye infections, and other conditions[18,19] and the leaves used in Indian folk medicine for diabetes mellitus.

Artemia salina (Brine shrimp) is commonly used to assess the cytotoxic effect of bioactive chemicals.[20] There is an imperative need to find out the antimalarial drug to develop safe and cheap new drugs against malarial parasites. The emergence of resistant strains demands to find out effective new drugs or drug combinations against malaria. In the present study, the efficacy of eco-friendly synthesized Au NPs was evaluated against *Plasmodium berghei* and the toxic effect tested against *A. salina*.

Materials and Methods

Sources

Chloroauric acid ($HAuCl_4$) was purchased from Sigma Aldrich, India. All other reagents used in the reaction were the analytical grade with maximum purity and glassware was washed with double distilled water and dried using the hot air oven.

Plant Collection

The fresh leaves of *C. grandis* were collected from Amirthi forest, Vellore District (12.7322° N, 79.0566° E) Tamil Nadu, India. The taxonomic identification was made by Dr. A. Akbar, Head, Department of Botany, C. Abdul Hakeem College (Autonomous), Melvisharam, Ranipet District. The voucher specimen was numbered (CAH/ZOO/AK/19/156) and kept in our research laboratory for further reference.

Synthesis of Au NPs

The fresh leaves of *C. grandis* were washed several times with distilled water to remove the dust particles and rinsed in deionized water. The extract was prepared from the thoroughly washed leaves (10 g) immersed in 100 mL of distilled water in an Erlenmeyer flask using a water bath, heated at 60°C for 5 min and monitored using UV-visible (UV-Vis) spectroscopy (Shimadzu 1601 spectrophotometer). Once the Au NPs was confirmed by their UV-Vis absorbance at 200–600 nm the reaction was stopped and centrifuged (Remi 2001) at 8000 rpm for 40 min. The supernatant liquid was discarded, and the resulting pellet was dispersed in deionized water. The centrifugation process was repeated 3–5 times to wash off any absorbed substances on the surface of Au NPs. The Au NPs were synthesized by reducing 1 mm of $HAuCl_4$ using 100 ml of 10% leaves extract at room temperature.[21]

Characterization of Au NPs

The biosynthesis of Au NPs was monitored by sampling the reaction mixture at regular intervals and the absorption maxima were scanned by UV-Vis spectra, at the wavelength of 200–700 nm and the spectra were recorded at 0 min, 30 min, 2 h and 4 h. Blanks were prepared for each of the samples with deionized water. The nano powder was subjected to X-ray diffraction (XRD) analysis (Phillips PW 1830 instrument) to determine the crystal structure, size and chemical composition of the Au NPs. X-ray generator, operated at a voltage of 40 kV and a current of 30 mA, wherein the sample was subjected to Cu radiations at 5°/min speed at a drive axis of 2θ and further, the images obtained were compared with the Joint Committee on Powder Diffraction Standards (JCPDS) library (file no: 04-0784) to account for the particle crystalline structure. Particle size was calculated using the obtained 2θ and d value.[22] The Fourier transform infrared (FTIR) analysis (Perkin Elmer spectrophotometer instrument) involved characterization of the dried powder of Au NPs by scanning it in the range 500–4000 cm^{-1} at a resolution of 4 cm^{-1}. The pellets were mixed with KBr powder and pelletized after drying properly. The pellets were later subjected to FTIR spectroscopy measurement were identified the functional groups. The size and morphological characterization of the Au NPs were studied using Scanning electron microscopic (SEM) studies (JEOL-JEM 6390, Japan) at ×10,000 magnifications operating with 20.00 kV. A thin film was prepared by drop coating biologically synthesized Au NPs onto carbon-coated copper SEM grids. The thin film on the SEM grid was allowed to stand for 5 min to dry before measurement and then the extra sample solution was removed using a blotting paper. Energy dispersive X-ray (EDX) spectroscopy analysis was determined the presence of gold, and the chemical composition of Au NPs. The sample was analyzed in Transmission electron microscopy (TEM, JEOL model 1200 EX), ultra-sonicated for 15 min, prepared on carbon-coated copper TEM grids for analysis and performed an instrument operated at an accelerating voltage of 120 kV and later with XDL 3000 powder. The selected area (electron) diffraction (SAED) pattern of the Au NPs is shown the presence of crystalline Au NPs as interpreted using the diffraction pattern.

In Vivo Antiplasmodial Activity

Experimental animal and parasite strain

Healthy male mice (Swiss albino mice) weighing 20–30 g at 6-weeks-old, obtained from the Institute of Veterinary Preventive Medicine, Ranipet, Tamil Nadu, India, were used for this study. The mice were grouped and housed in polyacrylic cages (38 × 23 × 10 cm) with three animals per cage and maintained under standard laboratory condition (the temperature at 27 ± 2°C with dark/light cycle 12:12 h). They were allowed a standard pellet diet (Hindustan Lever Limited, Mumbai, India) and clean drinking water ad libitum. The study was conducted under ethical committee permission and approval of the Government of India, Ministry of Environment and Forest, New Delhi, India (committee for control and supervision of experiments on animals; Reg. No. 1011/c/CPCSEA). The chloroquine (CQ)-sensitive *P. berghei* (NK 65) obtained from the National Institute of Malaria Research, New Delhi, India, was used to assess the *in vivo* intrinsic antimalarial activity.

Parasite inoculation

The Albino mice were infected with *P. berghei* and used as donor animals. The parasitemia of the donor mice was first determined and parasitized erythrocytes were obtained by cardiac puncture using anticoagulant and diluted in physiological saline (0.9%). The dilution was made based on the parasitemia of the donor mice and the RBC count of normal mice in such a way that 1 mL of blood contains 5×10^7 infected erythrocytes.[23] Each mouse was inoculated by intraperitoneal injection containing 1×10^7 parasitized erythrocytes (0.2 mL).

The 4-day suppressive assay

To evaluate the *in vivo* antimalarial activity of synthesized Au NPs using the leaves extracts of *C. grandis* against *P. berghei* infection in mice followed the procedure of Peter *et al*.[24] The infected mice were randomly divided into groups and the treatment was started 3 h after the mice had been inoculated with the parasite on Day 0. Treatment was then continued daily for 4 days from Day 0 to Day 3. They were then treated orally for 4 consecutive days with 50, 75 and 100 mg/kg body weight of the Au NPs. Two control groups were used; negative control (untreated control) was treated with distilled water, and positive control was treated with CQ 5 mg/kg. On day 4 of the experiment, tail blood was collected and thin blood film stained with Field's stain was examined under the microscope. The parasitemia was determined in blood smears that were characterized by random counting of 2000–4000 erythrocytes when parasitemia was low (≤10 %) or up to 1000 erythrocytes when parasitemia was higher. Parasitemia was constantly monitored up to cure or mortality. The mortality of mice was monitored daily in all groups during 4 weeks after inoculation.

% Parasitemia = Total number of parasitized RBCs/Total number of RBCs × 100

Parasitemia suppression was calculated using the following formula:

% suppression = Mean parasitemia of negative control–Mean parasitemia of treated group

Mean parasitemia of negative control × 100[25]

A. salina bioassay

The test was performed to predict the cytotoxic activity,[26] and the Au NPs were tested with different concentrations of 320, 160, 80, 40, 20 and 10 mg/ml. The 10 ml of sea water was added to the pre-labelled vials containing 10 live brine shrimp nauplii. After 24 h of incubation at room temperature (25–29°C), under continuous illumination of fluorescence lamp, the vials were inspected using a magnifying glass and the number of survived nauplii in each vial was counted. The mortality endpoint of this bioassay was defined as the absence of controlled forward motion during the 30s of observation.[27] The percent mortality of the brine shrimp nauplii for each concentration and control was calculated. The percentage of dead nauplii in the experiment was established by linear correlation when logarithm concentration versus percentage of mortality was plotted, and Lethal concentration (LC) values was calculated using Origin Pro[28] with minor modification.

Statistical Analysis

Statistical differences between the mean parasitemia of the control and experimental mice groups, percent inhibition on the 5th day of an experiment, as well as the range and mean survival time was assessed.[29] All values were expressed as mean ± standard deviation, with a limit of statistical significance of $P < 0.05$. The values were based on the drug concentrations along the X-axis. Statistical analyzes were done using origin 9.0.

Results and Discussion

UV-Vis Spectroscopy

The extracts of *C. grandis* was mixed in the aqueous solution of the Au^+ ions complex, and it started to change the color from light yellow to ruby pink due to the reduction of Au^+ ions which indicated the formation of Au NPs. The control showed no color change. The UV-vis spectra indicated a surface plasmon resonance (SPR) gold band at 500–600 nm and the intensity steadily increased to saturation as a function of the recorded spectra at different time intervals such as 0 min, 30 min, 2 h and 4 h are shown in different reaction time [Figure 1]. The time required for the complete conversion of Au^+ to Au NPs was 4 h. The previous authors reported that the synthesized Au NPs using *Madhuca longifolia*[30] and *T. decandra*[14] required 2 h and 3 h, respectively. The obtained Au NPs were stable for a period of 2 months due to the coordination of carbonyl groups of oxidized polyphenols onto the surface of Au NPs.

The extract concentration is an affecting factor in the intensity of the extinction peak of synthesized NPs spectra. A significant increase in the intensity of the SPR peak of Au NPs occurs in the presence of the extract, which may indicate a formation of a maximum number of Au NPs due to a decrease in the agglomeration and higher nucleation.[14,30] Extract molecules can protect the particles from aggregation and the probability of NPs collision and coalescence decreases due to the reaction between functional groups of stabilizer and NPs.[31] When the size of Au NPs decreases, there is an increase in the number of low-coordinated Au atoms which promote the absorption of the reactants on the catalyst surface and facilitates the reduction.[32,33] The UV-vis spectra of Au NPs at other ratios have broad peaks with low intensities which might be due to the formation of large anisotropic particles. The SPR absorbance is extremely sensitive to the nature, size and shapes of the particles formed and their inter-particle distances.[34] Furthermore, the size and the concentration of Au NPs can be determined directly from UV-vis spectra.[35,36] The larger NPs with sizes of approximately 18 and 20 nm; the distance between adjacent NPs is considerably smaller than the size of the NPs; therefore, obvious changes in the spectrophotometric properties of NPs and the consequent color of the solution was observed. These results confirm with the previously reported studies on the leaves extract of *C. auriculata* with $HAuCl_4$ transmuted color rapidly from pale yellow to ruby red, indicating the formation of Au NPs (with a diameter less than 25 nm) due to the localized SPR.[13] It may be attributed to a secondary reduction phenomenon on the surface of preformed nuclei, which becomes more pronounced as the extract concentration rises.

XRD Analysis

XRD analysis of synthesized Au NPs using *C. grandis* showed in the form of nanocrystals, as evidenced by the peaks at 2θ values of 26.88°, 27.98°, 29.13°, 40.14°, 42.88°, 49.82°, and 66.01°

correspond to the (200), (102), (112), (022), (310), (113), and (223) Bragg's plane of face cantered cubic (fcc) gold lattice, respectively, which are in agreement with the diffraction standard of gold (JCPDS) [Figure 2]. In this case, the peak due to (102) reflection was more intense than those owed to (223) and (022) reflections, suggesting that the synthesized Au NPs were nanocrystalline in nature. This clearly reported that Au NPs were predominantly oriented along the (111) plane utilizing *C. grandis* extracts. The unassigned peaks crystallization due to the bioorganic phase surface of the NPs. Similar patterns of XRD have been reported form the synthesized Au NPs using the extracts of *Nyctanthes arbortristis* showed 38.10, 44.40, 64.80 and 78.0 corresponding to the (111), (200), (220) and (311) planes of fcc lattice structure of gold.[37] Similarly, the crystalline nature of Au NPs synthesized from the extracts of *C. auriculata*, the XRD showed three diffraction peaks at the 2θ range of 30–80°, which can be indexed as (111), (200), (220) reflections of fcc structure metallic gold, respectively.[13]

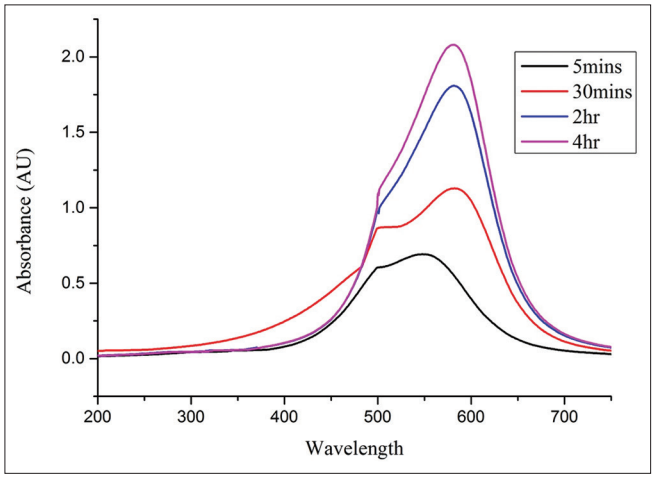

Figure 1: UV-visible spectra of synthesized gold nanoparticles using the aqueous leaves extracts of *Coccinia grandis*

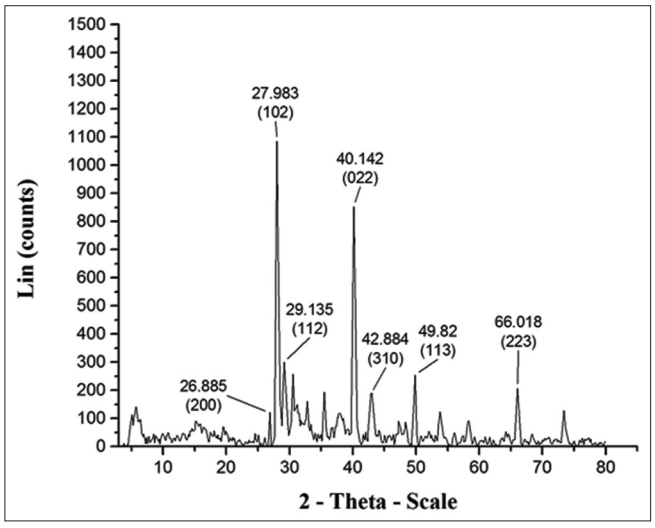

Figure 2: X-ray diffraction diffractograms of synthesized gold nanoparticles using the *Coccinia grandis*

FTIR Spectroscopy

FTIR analysis was performed to identify the possible biomolecules responsible for the reduction of the Au^{+} ions and capping of the reduced Au NPs synthesized by plant leaves extract [Figure 3]. Results of the present study revealed that the functional groups for the synthesized Au NPs showed the presence of bands due to O-H Hydroxy group, H-bonded OH stretch (3274 cm^{-1}), N-H Primary amine, NH bend (1637 cm^{-1}), O-H Phenol or tertiary alcohol, OH bend (1406 cm^{-1}), Skeletal C-C vibrations (1272 cm^{-1}), C-F Aliphatic fluoro compounds, C-F stretch (1094 cm^{-1}), C-O-O-C Peroxides, C-O-O-stretch (867 cm^{-1}), C-I Aliphatic iodo compounds, C-I stretch (546 cm^{-1}) and Aryl disulfides (S-S stretch) corresponds to 463 cm^{-1}. This suggests the loss of the OH intramolecular hydrogen bond functional group which might be responsible for the reduction of Au^{+} to Au^{0}.[38,39] The polypeptides or proteins had rich amino and thiol groups, which strongly bind the Au (0), forming a polypeptides/protein-Au complex. The reduction function of the amino acid residues was activated to trigger the nucleation and growth of Au NPs in the scaffolds between amino acid molecules. These structural changes have confirmed the fact that the polypeptides or proteins could possibly form a layer covering the NPs to prevent agglomeration and thereby stabilize the medium.[40-42] Our analysis confirms the findings of the previous authors report, the FTIR spectrum of synthesized Au NPs from *M. tenuiflora* showed the characteristic broad bands at 3250 cm^{-1} were associated with phenolic OH from tannins and flavonoids mainly, the peak at 1594 cm^{-1} correspond to N-H bending vibration, and the 1705 cm^{-1} to ketone acyclic stretch and region between 1000 and 1300 cm^{-1} to C–O stretch.[16] It can be suggested that the water-soluble fractions in the biomass played an important role in the bioreduction and shape evolution of the NPs. The changes in the FTIR peaks in the present study were a confirmation of the interaction of the different plant components with $HAuCl_4$ solution.

SEM and Energy Dispersive Spectrum (EDS) Analysis

SEM analysis confirmed the cubical structure of the synthesized Au NPs, which had an average size of 24.23 ± 31 nm and were

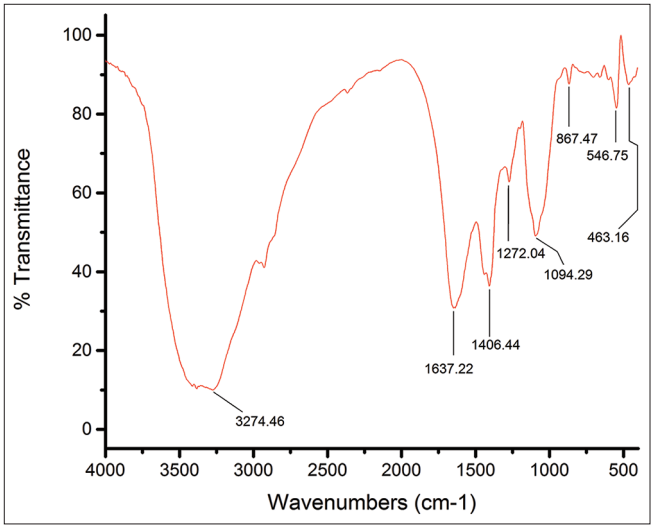

Figure 3: Fourier transform infrared spectrum of synthesized gold nanoparticles using the *Coccinia grandis* leaves extracts

produced during bioreduction of $HAuCl_4$, which could have contained chloride ions. The synthesized Au NPs were found to be square, with equal dimensions on all sides, the reason might be the crystallization of $HAuCl_4^-$ ions as shown in Figure 4. The presence of gold atoms in the Au NPs was further confirmed by EDX spectroscopy. The optical absorption peak formed at approximately 3.3 keV, which is typical of gold nano crystallite absorption due to SPR. The EDS analysis displays a strong major peak for Au; the remaining weaker signals were recorded possibly due to elements (Al, C and O) from organic moieties and the grid used for this analysis. The energy dispersive spectrum profile of Au NPs using *C. grandis* extract [Figure 4] showed strong gold atom signals around 3–4 keV. The EDS analysis of the chemical composition of $HAuCl_4$ ions treated extracted mediated synthesis of Au NPs showed spectral peaks corresponding to gold atoms. The high-intensity bands for carbon and oxygen revealed the presence of bioorganic components such as proteins and other macromolecules along with gold atoms in the sample. Similar results were reported from the synthesized Au NPs using the leaves extract of *Stevia rebadiauna*, the SEM micrographs were spherical in shape with sizes ranging from 21 to 45 nm, EDS strong signals were observed from the gold atoms and weaker signals for carbon, oxygen, potassium and chloride were prevenient from biomolecules of *S. rebadiauna*.[43]

TEM with SAED Analysis

The TEM image reveals the formation of isotropic and spherical and oval shape, which corresponds to the shape from the SPR band in the UV-Vis spectra. The result obtained from the TEM study clearly indicates the shape and size of the NPs and illustrates the individual NPs as well as the clusters. The fringes of the Au NPs as shown in Figure 5 and confirmed the nanocrystalline nature of the NPs. The synthesized Au NPs using *C. grandis* obtained were fairly dispersed, ranging between 2–50 nm, with an average size of 2.82 ± 2.5 nm, spherical and oval-shaped particles with a homogenous distribution. The synthesized Au NPs using *C. grandis* obtained were fairly dispersed showed an average size of 2.82 ± 2.5 nm. A few agglomerated Au NPs were observed in some places of the TEM micrograph, they were not involved in direct contact due to the presence of a capping agent. The crystalline structures of synthesized NPs were further confirmed by their corresponding SAED analysis as indicated in Figure 5d. Earlier authors reported that the TEM images of synthesized Au NPs from the extracts of *C. auriculata* showed spherical, hexagonal and triangular shape with an average size of 17 nm.[13] Recently, Rodríguez-León *et al.*[16] reported that the TEM images for the synthesis of Au NPs from *M. tenuiflora* showed an average size of 40 nm.

In Vivo Antiplasmodial Activity

After being inoculated intraperitoneally of *P. berghei* ANKA with 1×10^7 infection in Swiss mice, Field's staining of thin blood smear was performed and microscopic examination of the untreated group showed >30% parasitemia on day 4, survival period of animals without treatment was poor with percent survival. The experimental group showed a reduction of mean parasitemia (%) on day 4 after being treated with *C. grandis* leaves extract and $HAuCl_4$ solution showed 12.96 ± 1.13 and 14.75 ± 0.73, respectively, at 75 mg/kg body weight. The synthesized Au NPs using the leaves extracts of *C. grandis* showed 10.51 ± 0.93, 8.25 ± 0.67, and 6.67

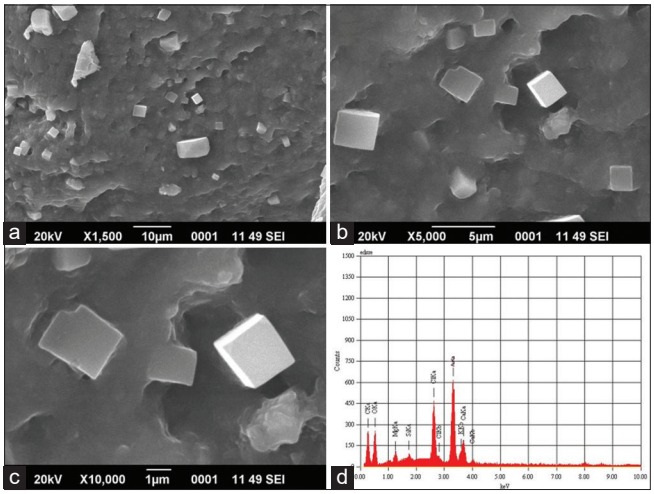

Figure 4: Scanning electron microscopic images of synthesized gold nanoparticles using the *Coccinia grandis* leaves extract. Magnification at (a) ×1,500, (b) ×5,000, (c) ×10,000, (d) EDS

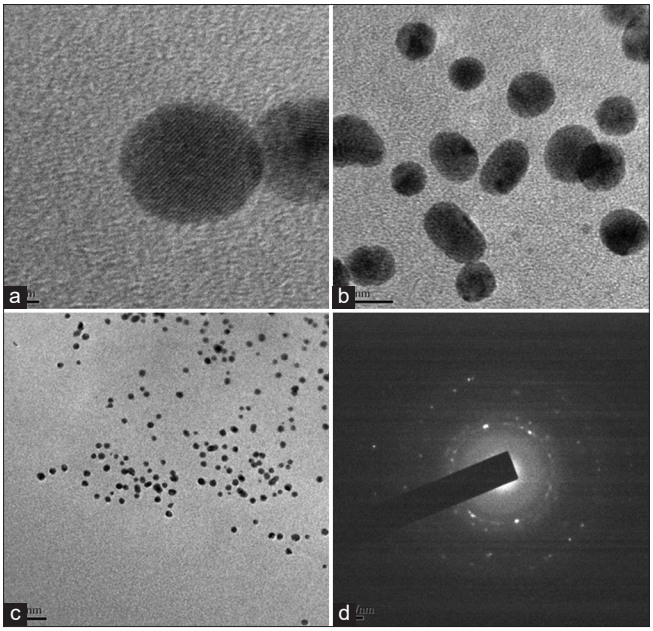

Figure 5: Transmission electron microscopy images of synthesized gold nanoparticles using the *Coccinia grandis* leaves extract (a) 2 nm, (b) 10 nm, (c) 50 nm and (d) SAED pattern scale at 5.1 nm

± 0.79% at 50, 75, and 100 mg/kg body weight, respectively [Figure 6 and Table 1]. The CQ was tested in a parallel test which parasitemia 0.76 ± 0.08% at 5 mg/kg/body weight. The doses and efficacy were tested for parasite suppression and parasitemia was observed on day 4 for the synthesized Au NPs using *C. grandis* extracts showed 69.45, 76.02 and 80.61%, respectively, at 50, 75 and 100 mg/kg body weight [Table 2]. Earlier authors reported that the percentage of parasitemia suppression for the synthesis of Au NPs using *Streptomyces* sp (Au-NLK3) were 40% at 8 mg/kg.[44]

The parasitemia of infected mice treated with Au-CQ at a dose of 1mg per kg body weight was reduced by 84% when compared to untreated controls, whereas the parasitemia of mice treated with an equivalent concentration of chloroquine diphosphate was reduced by only 44%, indicating that complexation of Au to

Table 1: The survival and parasitemia progress of synthesized Au NPs using the *C. grandis* leaves extract against ANKA strains of *P. berghei* infected mice

Groups	*% Parasitemia (Mean±S.D) (Number of Days)*				
	1	*4*	*6*	*8*	*10*
C. grandis 75 mg/kg	0.65±0.08 (6/6)	12.96±1.13 (6/6)	58.09±1.64 (4/6)	63.33±1.27 (2/6)	76.43±0.00 (1/6)
$HAuCl_4$ 75 mg/kg	0.78±0.12 (6/6)	14.75±0.73 (6/6)	52.15±1.81 (3/6)	58.41±1.63 (3/6)	71.34±0.00 (1/6)
Au NPs 50 mg/kg	0.53±0.06 (6/6)	10.51±0.93 (6/6)	42.56±1.40 (4/6)	46.44±1.29 (4/6)	66.04±1.52 (2/6)
Au NPs 75 mg/kg	0.45±0.04 (6/6)	8.25±0.67 (6/6)	32.47±1.53 (4/6)	40.27±1.28 (4/6)	46.17±1.34 (2/6)
Au NPs 100 mg/kg	0.36±0.03 (6/6)	6.67±0.79 (6/6)	26.89±1.79 (5/6)	36.03±1.13 (6/6)	42.34±1.10 (2/6)
Negative control	3.2±0.48 (6/6)	34.41±1.61 (6/6)	88.45±0.00 (1/6)	92.46±0.00 (1/6)	(0)
Chloroquine (Positive control) 5 mg/kg	0.00±0.00 (6/6)	0.76±0.08 (6/6)	1.91±0.18 (6/6)	2.78±0.50 (6/6)	4.99±0.74 (6/6)

For each group *n*=6. Parenthesis: (Number of live mice/Total number of mice infected). *C. grandis: Coccinia grandis, P. berghei: Plasmodium berghei*, Au NPs: Gold nanoparticles, $HAuCl_4$: Chloroauric acid

Table 2: The % Suppression progress of synthesized Au NPs using the *C. grandis* leaves extract against ANKA strains of P. berghei infected mice

Groups	*% Suppression (Number of Days)*				
	1	*4*	*6*	*8*	*10*
C. grandis	79.68	62.33	34.32	31.50	23.57
50 mg/kg Au NPs	83.43	69.45	51.88	49.77	33.96
75 mg/kg Au NPs	85.93	76.02	63.28	56.44	53.83
100 mg/kg Au NPs	88.75	80.61	69.59	61.03	57.66
Negative control	96.8	65.59	11.55	7.54	0
Chloroquine 5 mg/kg (Positive control)	100	97.79	97.84	96.99	95.01

C. grandis: Coccinia grandis, P. berghei: Plasmodium berghei, Au NPs: Gold nanoparticles

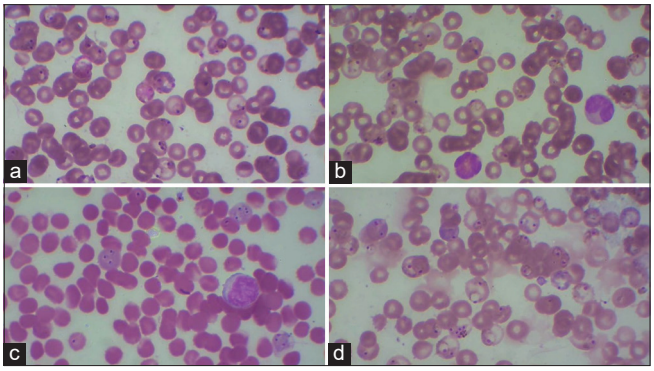

Figure 6: *In vivo* antimalarial activity of synthesized gold nanoparticles tested against ANKA strain of *Plasmodium berghei* at different concentration (a) 50, (b) 75, (c) 100 mg/kg and (d) negative control

CQ significantly increased the *in vivo* susceptibility of *P. berghei*. No apparent adverse reactions or apparent acute toxic responses were observed.[45] Malaria infected mice suffer from anemia because of erythrocyte destruction, either by malaria multiplication or by spleen reticuloendothelial cell action.[46] An ideal antimalarial candidate should prevent anemia secondary to preventing hemolysis, body temperature reduction and weight loss in mice. In this study, a significant attenuation of body temperature reduction and Packed cell volume was observed by synthesized Au NPs using *C. grandis* extracts at 50 and 100 mg/kg doses. This was also comparable to the commonly used drug chloroquine. According to our findings, the antiplasmodial activity of biosynthesized nano-formulations may be due to the presence of bioactive metabolites, which may confer protective properties against oxidative stress caused by malarial parasites in the host's parasitized red blood cells.

Brine Shrimp Lethality Bioassay

In the brine shrimp lethality bioassay, 50% mortality rate (LC_{50}) values <150 µg/ml were considered significantly active and potentially lethal. The LC values for synthesized Au NPs from *C. grandis* showed that the LC_{20}, LC_{50}, and LC_{90} values were 89.66, 135.05, and 258.49 µg/mL, respectively [Figure 7]. In agreement with our results, Balalakshmi *et al*.[47] previously reported that the synthesized Au NPs using leaves extract of *Sphaeranthus indicus* showed no mortality on *Artemia nauplii*, all the tested animals showed 100% survivability. In addition, Kesarla *et al*.[48] reported

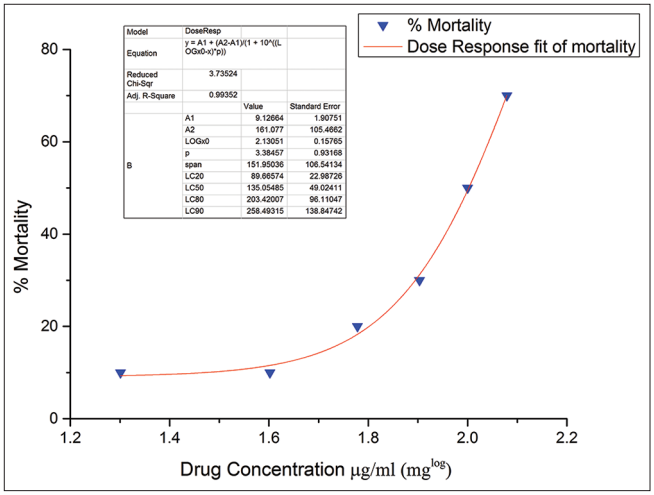

Figure 7: The LC_{20}, LC_{50}, LC_{80} and LC_{90} values of synthesized gold nanoparticles against the brine shrimp (*Artemia salina*) larvae

that the synthesized Au NPs from *Terminalia bellirica* extracts did not show any toxicity up to 1000 mg/L tested by the brine shrimp (*A. salina*) assay. Because of their non-toxic nature, these Au NPs can be used in a wide range of biological and medical applications.

Conclusion

Antimalarial drugs have been the mainstay of control and prophylaxis against malaria since the first use of quinine from the cinchona tree. Many drugs were developed against malaria in the 20th century with the most important being chloroquine and artemisinin. However, the ability of *Plasmodium* in particular to develop resistance to these treatments has threatened their continuing efficacy and raised the importance of combinations as well as developing new drugs and novel targets. The present study shows that the synthesized Au NPs using the aqueous leaves extract of *C. grandis* possess good antimalarial activity. No adverse effect was noticed when the extract and synthesized NPs were orally administered, alluding that the extract is not acutely toxic when administered to mice through this route. This supports its use in ethnomedicine in the treatment of malaria. Furthermore, it demonstrates its potential as a source of an antimalarial drug molecule. However, the findings are only preliminary, therefore, confirmatory studies, followed by isolation and characterization of the active antimalarial compound(s) responsible for the observed curative activity are recommended.

Acknowledgments

We are grateful to the Management of C. Abdul Hakeem College (Autonomous), Melvisharam, Affiliated to Thiruvalluvar University, Vellore, Principal and HOD of Post Graduate and Research Department of Zoology for providing the facilities to carry out this work. K. Anbarasan gratefully thanks to Department of Biotechnology (BT/PR936/PBD/17/740/2011) Government of India, New Delhi, for the Junior Research Fellowship.

Copyright and Permission Statement

References

1. World Health Organization. Fact Sheet About Malaria. Geneva: World Health Organization; 2020.
2. World Health Organization. High Burden to High Impact: A Targeted Malaria Response. Geneva: World Health Organization; 2018.
3. Ghosh SK, Rahi M. Malaria elimination in India-the way forward. J Vector Borne Dis 2019;56:32.
4. Nualkaew S, Rattanamanee K, Thongpraditchote S, Wongkrajang Y, Nahrstedt A. Anti-inflammatory, analgesic and wound healing activities of the leaves of *Memecylon edule* Roxb. J Ethnopharmacol 2009;121:278-81.
5. Mandal D, Bolander ME, Mukhopadhyay D, Sarkar G, Mukherjee P. The use of microorganisms for the formation of metal nanoparticles and their application. Appl Microbiol Biotechnol 2006;69:485-92.
6. Armendariz V, Herrera I, Jose-yacaman M, Troiani H, Santiago P, Gardea-Torresdey JL. Size controlled gold nanoparticle formation by *Avena sativa* biomass: Use of plants in nanobiotechnology. J Nanoparticle Res 2004;6:377-82.
7. Jain PK, Huang X, El-Sayed IH, El-Sayed MA. Noble metals on the nanoscale: Optical and photothermal properties and some applications in imaging, sensing, biology, and medicine. Acc Chem Res 2008;41:1578-86.
8. Cheng Y, Samia AC, Meyers JD, Panagopoulos I, Fei B, Burda C. Highly efficient drug delivery with gold nanoparticle vectors for *in vivo* photodynamic therapy of cancer. J Am Chem Soc 2008;130:10643-7.
9. Sperling RA, Gil PR, Zhang F, Zanella M, Parak WJ. Biological applications of gold nanoparticles. Chem Soc Rev 2008;37:1896-908.
10. Hainfeld JF, Slatkin DN, Focella TM, Smilowitz HM. Gold nanoparticles: A new X-ray contrast agent. Br J Radiol 2006;79:248-53.
11. Chandran SP, Chaudhary M, Pasricha R, Ahmad A, Sastry M. Synthesis of gold nanotriangles and silver nanoparticles using *Aloe vera* plant extract. Biotechnol Prog 2006;22:577-83.
12. Mohanpuria P, Rana NK, Yadav SK. Biosynthesis of nanoparticles: Technological concepts and future applications. J Nanoparticle Res 2008;10:507-17.
13. Kumar VG, Gokavarapu SD, Rajeswari A, Dhas TS, Karthick V, Kapadia Z, *et al*. Facile green synthesis of gold nanoparticles using leaf extract of antidiabetic potent *Cassia auriculata*. Coll Surf B Biointerf 2011;87:159-63.
14. Geethalakshmi R, Sarada DV. Gold and silver nanoparticles from *Trianthema decandra*: Synthesis, characterization, and antimicrobial properties. Int J Nanomedicine 2012;7:5375.
15. Ghramh HA, Khan KA, Ibrahim EH, Setzer WN. Synthesis of gold nanoparticles (AuNPs) using *Ricinus communis* leaf ethanol extract, their characterization, and biological applications. Nanomaterials 2019;9:765.
16. Rodríguez-León E, Rodríguez-Vázquez BE, Martínez-Higuera A, Rodríguez-Beas C, Larios-Rodríguez E, Navarro RE, *et al*. Synthesis of gold nanoparticles using *Mimosa tenuiflora* extract, assessments of cytotoxicity, cellular uptake, and catalysis. Nanoscale Res Lett 2019;14:1-16.
17. Dash SS, Majumdar R, Sikder AK, Bag BG, Patra BK. *Saraca indica* bark extract mediated green synthesis of polyshaped gold nanoparticles and its application in catalytic reduction. Appl Nanosci 2014;4:485-90.
18. Subramaniam J, Murugan K, Panneerselvam C, Kovendan K, Madhiyazhagan P, Dinesh D, *et al*. Multipurpose effectiveness of *Couroupita guianensis*-synthesized gold nanoparticles: High antiplasmodial potential, field efficacy against malaria vectors and synergy with *Aplocheilus lineatus* predators. Environ Sci Pollut Res 2016;23:7543-58.
19. Dhote P. Antibacterial and hypoglycemic activity of *coccinia grandis* (L.) voigt plant. Delta Natl J Multidiscip Res 2018;5:64-70.
20. Wu C. An important player in brine shrimp lethality bioassay: The solvent. J Adv Pharm Technol Res 2014;5:57.
21. Annamalai A, Christina VL, Sudha D, Kalpana M, Lakshmi PT. Green synthesis, characterization and antimicrobial activity of Au NPs using *Euphorbia hirta* L. leaf extract. Coll Surf B Biointerf 2013;108:60-5.
22. Ebrahimzadeh MA, Naghizadeh A, Mohammadi-Aghdam S, Khojasteh H, Ghoreishi SM, Mortazavi-Derazkola S. Enhanced catalytic and antibacterial efficiency of biosynthesized *Convolvulus fruticosus* extract capped gold nanoparticles (CFE@ AuNPs). J Photochem Photobiol B Biol 2020;209:111949.
23. Ljungström I, Moll K, Perlmann H, Scherf A, Wahlgren M. Methods in Malaria Research. United States: MR4/ATCC; 2008.
24. Peters W, Portus JH, Robinson BL. The four-day suppressive *in vivo* antimalarial test. Ann Trop Med Parasitol 1975;69:155-71.
25. Kalra BS, Chawla S, Gupta P, Valecha N. Screening of antimalarial drugs: An overview. Indian J Pharmacol 2006;38:5.
26. Meyer BN, Ferrigni NR, Putnam JE, Jacobsen LB, Nichols DE, McLaughlin JL. Brine shrimp: A convenient general bioassay for active plant constituents. Planta Med 1982;45:31-4.
27. Middleton P, Stewart F, Al-Qahtani S, Egan P, O'Rourke C, Abdulrahman A, *et al*. Antioxidant, antibacterial activities and general toxicity of *Alnus glutinosa*, *Fraxinus excelsior* and *Papaver rhoeas*. Iran J Pharm Res 2010;2:101-3.
28. Pervin R, Afrin S, Sabrin F, Zohora US, Rahman MS, Islam KD, *et al*. Antioxidant, antibacterial and brine shrimp lethality bioassay of *Amoora cucullata*, a Mangrove plant. J Young Pharm 2016;8:33.
29. Rajakumar G, Rahuman AA, Chung IM, Kirthi AV, Marimuthu S,

Anbarasan K. Antiplasmodial activity of eco-friendly synthesized palladium nanoparticles using *Eclipta prostrata* extract against *Plasmodium berghei* in Swiss albino mice. Parasitol Res 2015;114:1397-406.
30. Sharma M, Yadav S, Ganesh N, Srivastava MM, Srivastava S. Biofabrication and characterization of flavonoid-loaded Ag, Au, Au-Ag bimetallic nanoparticles using seed extract of the plant *Madhuca longifolia* for the enhancement in wound healing bio-efficacy. Prog Biomater 2019;8:51-63.
31. Li Y, Zhang J, Gu J, Chen S. Biosynthesis of polyphenol-stabilised nanoparticles and assessment of anti-diabetic activity. J Photochem Photobiol B Biol 2017;169:96-100.
32. Sharma RK, Gulati S, Mehta S. Preparation of gold nanoparticles using tea: A green chemistry experiment. J Chem Educ 2012;89:1316-8.
33. Aromal SA, Philip D. Green synthesis of gold nanoparticles using *Trigonella foenum-graecum* and its size-dependent catalytic activity. Spectrochim Acta Part A Mol Biomol Spectrosc 2012;97:1-5.
34. Sun Y, Xia Y. Increased sensitivity of surface plasmon resonance of gold nanoshells compared to that of gold solid colloids in response to environmental changes. Anal Chem 2002;74:5297-305.
35. Haiss W, Thanh NT, Aveyard J, Fernig DG. Determination of size and concentration of gold nanoparticles from UV-Vis spectra. Anal Chem 2007;79:4215-21.
36. Murphy CJ, Gole AM, Hunyadi SE, Stone JW, Sisco PN, Alkilany A, *et al*. Chemical sensing and imaging with metallic nanorods. Chem Commun 2008;5:544-57.
37. Das RK, Gogoi N, Bora U. Green synthesis of gold nanoparticles using *Nyctanthes arbortristis* flower extract. Bioprocess Biosyst Eng 2011;34:615-9.
38. Dubey SP, Lahtinen M, Sillanpää M. Tansy fruit mediated greener synthesis of silver and gold nanoparticles. Process Biochem 2010;45:1065-71.
39. Priyadarshini S, Gopinath V, Priyadharsshini NM, MubarakAli D, Velusamy P. Synthesis of anisotropic silver nanoparticles using novel strain, *Bacillus flexus* and its biomedical application. Coll Surf B Biointerf 2013;102:232-7.
40. Sathishkumar G, Jha PK, Vignesh V, Rajkuberan C, Jeyaraj M, Selvakumar M, *et al*. Cannonball fruit (*Couroupita guianensis*, Aubl.) extract mediated synthesis of gold nanoparticles and evaluation of its antioxidant activity. J Mol Liq 2016;215:229-36.
41. Raghavan BS, Kondath S, Anantanarayanan R, Rajaram R. Kaempferol mediated synthesis of gold nanoparticles and their cytotoxic effects on MCF-7 cancer cell line. Process Biochem 2015;50:1966-76.
42. Islam NU, Jalil K, Shahid M, Muhammad N, Rauf A. *Pistacia integerrima* gall extract mediated green synthesis of gold nanoparticles and their biological activities. Arab J Chem 2019;12:2310-9.
43. Sadeghi B, Mohammadzadeh M, Babakhani B. Green synthesis of gold nanoparticles using *Stevia rebaudiana* leaf extracts: Characterization and their stability. J Photochem Photobiol B Biol 2015;148:101-6.
44. Karthik L, Kumar G, Keswani T, Bhattacharyya A, Reddy BP, Rao KV. Marine actinobacterial mediated gold nanoparticles synthesis and their antimalarial activity. Nanomed Nanotechnol Biol Med 2013;9:951-60.
45. Navarro M, Pérez H, Sánchez-Delgado RA. Toward a novel metal-based chemotherapy against tropical diseases. 3. Synthesis and antimalarial activity *in vitro* and *in vivo* of the new gold-chloroquine complex [Au (PPh3)(CQ)] PF6. J Med Chem 1997;40:1937-9.
46. Chinchilla M, Guerrero OM, Abarca G, Barrios M, Castro O. An *in vivo* model to study the anti-malaric capacity of plant extracts. Rev Biol Trop 1998;46:35-9.
47. Balalakshmi C, Gopinath K, Govindarajan M, Lokesh R, Arumugam A, Alharbi NS, *et al*. Green synthesis of gold nanoparticles using a cheap *Sphaeranthus indicus* extract: Impact on plant cells and the aquatic crustacean *Artemia nauplii*. J Photochem Photobiol B Biol 2017;173:598-605.
48. Kesarla MK, Mandal BK, Bandapalli PR. Gold nanoparticles by *Terminalia bellirica* aqueous extract-a rapid green method. J Exp Nanosci 2014;9:825-30.